

## Supplementary Information

### **Manganese-doped gold core mesoporous silica particles as a nanoplatfom for dual-modality imaging and chem- chemodynamic combination osteosarcoma therapy**

Zhou Sha<sup>†</sup>, Shuguang Yang<sup>†</sup>, Liwen Fu<sup>†</sup>, Mengru Geng<sup>†</sup>, Jiani Gu<sup>†</sup>, Xuying Liu<sup>†</sup>, Shikai Li<sup>†</sup>, Xiaojun Zhou<sup>†,\*</sup>, Chuanglong He<sup>†,\*</sup>

<sup>†</sup> State Key Laboratory for Modification of Chemical Fibers and Polymer Materials, College of Chemistry, Chemical Engineering and Biotechnology, Donghua University, Shanghai 201620, China.

Correspondence to: hcl@dhu.edu.cn

## **Supplementary Experimental Section:**

### **Characterization**

The morphology and structure of Au@MMSN-Ald were observed with transmission electron microscopy (TEM) operating at 200 kV (JEM-2100, JEOL Ltd., Japan). The surface areas and average pore size distributions of nanoparticles were calculated by Brunauer–Emmett–Teller (BET) and Barrett–Jyner–Halenda (BJH) methods. Element mappings were acquired by field-emission transmission electron microscopy (Talos F200S). The Fourier transform infrared (FTIR) spectrum was recorded by a Nexus 670 (Thermo Nicolet, USA) spectrometer and examined by KBr pellets. X-ray photoelectron spectroscopy (XPS) was used to analyze the valence state of covalent compounds (Escalab 250Xi, USA). The X-ray diffraction (XRD) was obtained by D/max-2550VB+/PC\* (RIGAKU, Japan). Computed Tomography (CT) scanning was performed using a dual-source SOMATOM Definition Flash CT system (Siemens, Erlangen, Germany) with 140 KV. Dynamic light scattering (DLS) was used to estimate the size distribution of the nanoparticles using a BI-200SM multiangle dynamic/static laser scattering instrument (Brookhaven, U.S.). Zeta-potential was examined by a Zetasizer Nano ZS apparatus (Malvern Instruments, UK). The surface areas and average pore size distributions of nanoparticles were calculated by Brunauer–Emmett–Teller (BET) and Barrett–Jyner–Halenda (BJH) methods. Thermogravimetric (TG) analysis was performed by using a TG 209 F1 (NETZSCH Instruments Co., Ltd., Germany) thermogravimetric analyzer. The quantitative measurements of Mn and Si were determined by Leeman Prodigy inductively coupled plasmaatomic emission spectroscopy (ICP-AES, Hudson, NH03051, USA).

**Supplementary Figures:**

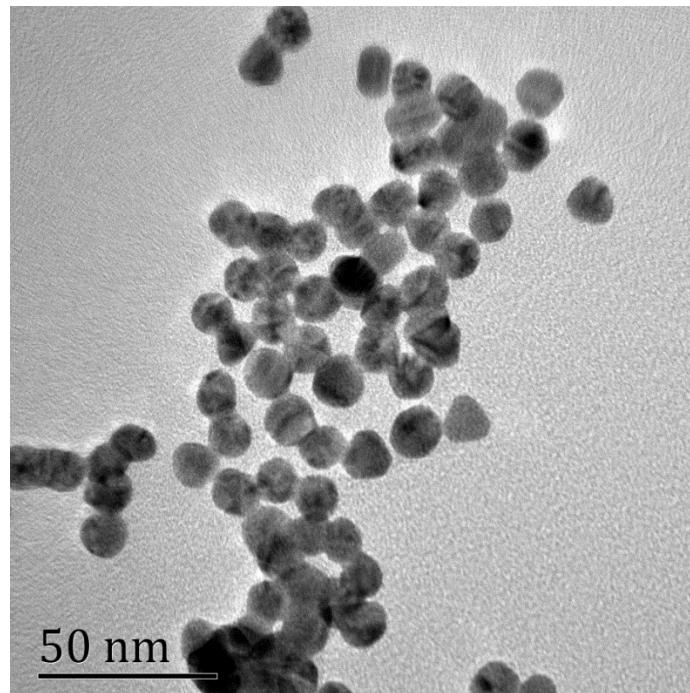


**Fig. S1** TEM image of Au nanoparticles.

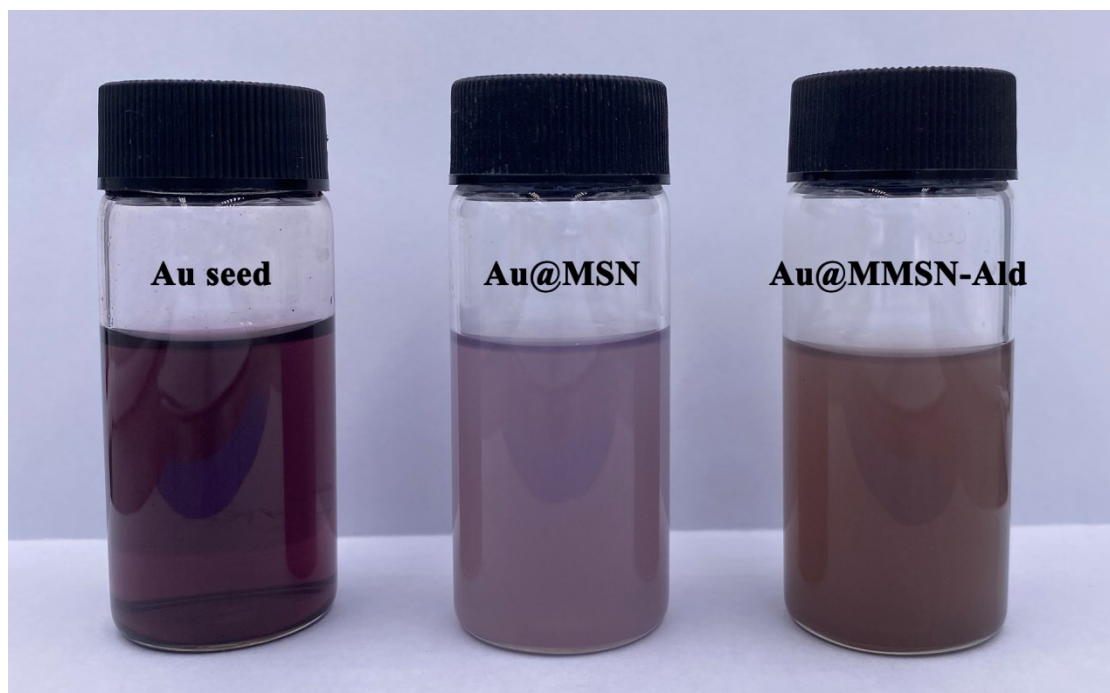


**Fig. S2** The photographs of Au seed, Au@MSN and Au@MMSN-Ald nanoparticles dispersed in water.

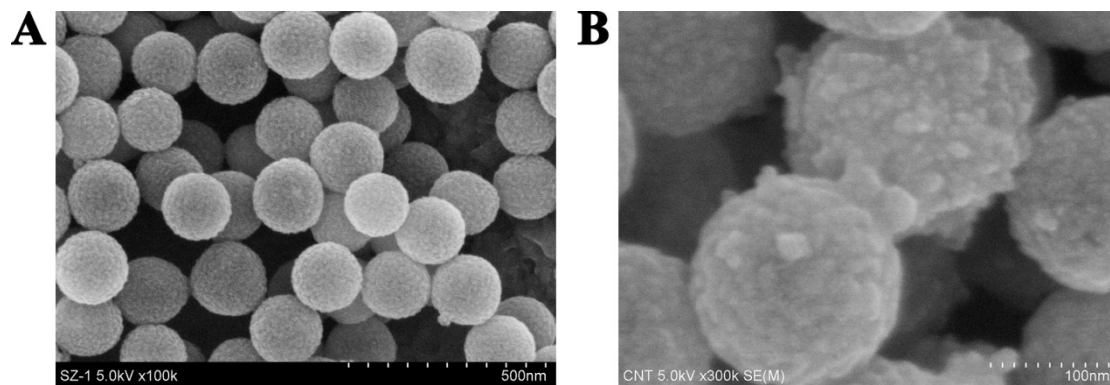


**Fig. S3** SEM images of (A) Au@MSN and (B) Au@mMSN-Ald.

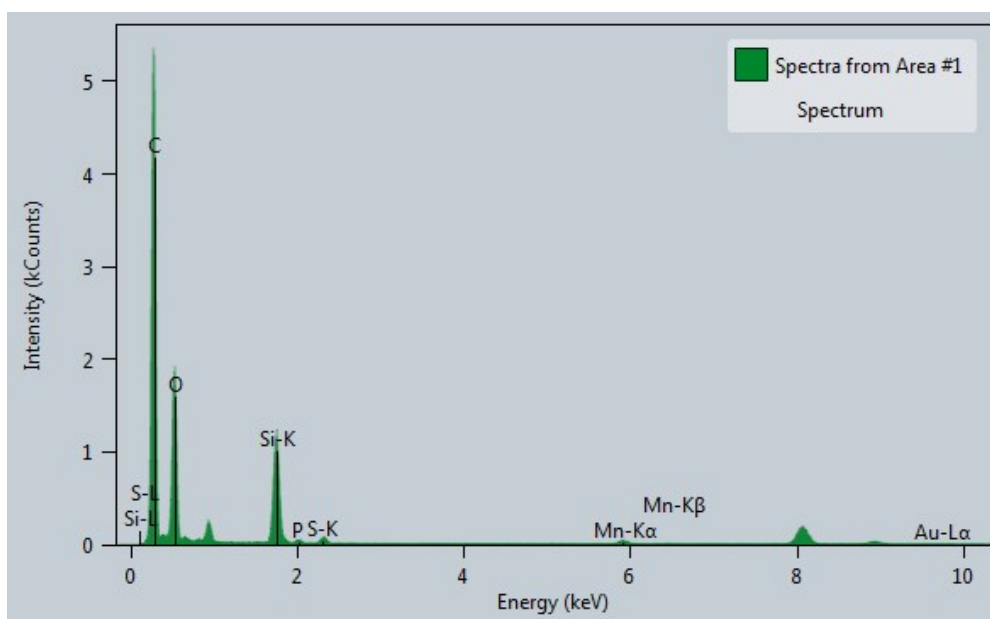


**Fig. S4** EDS spectrum of Au@mMSN-Ald.

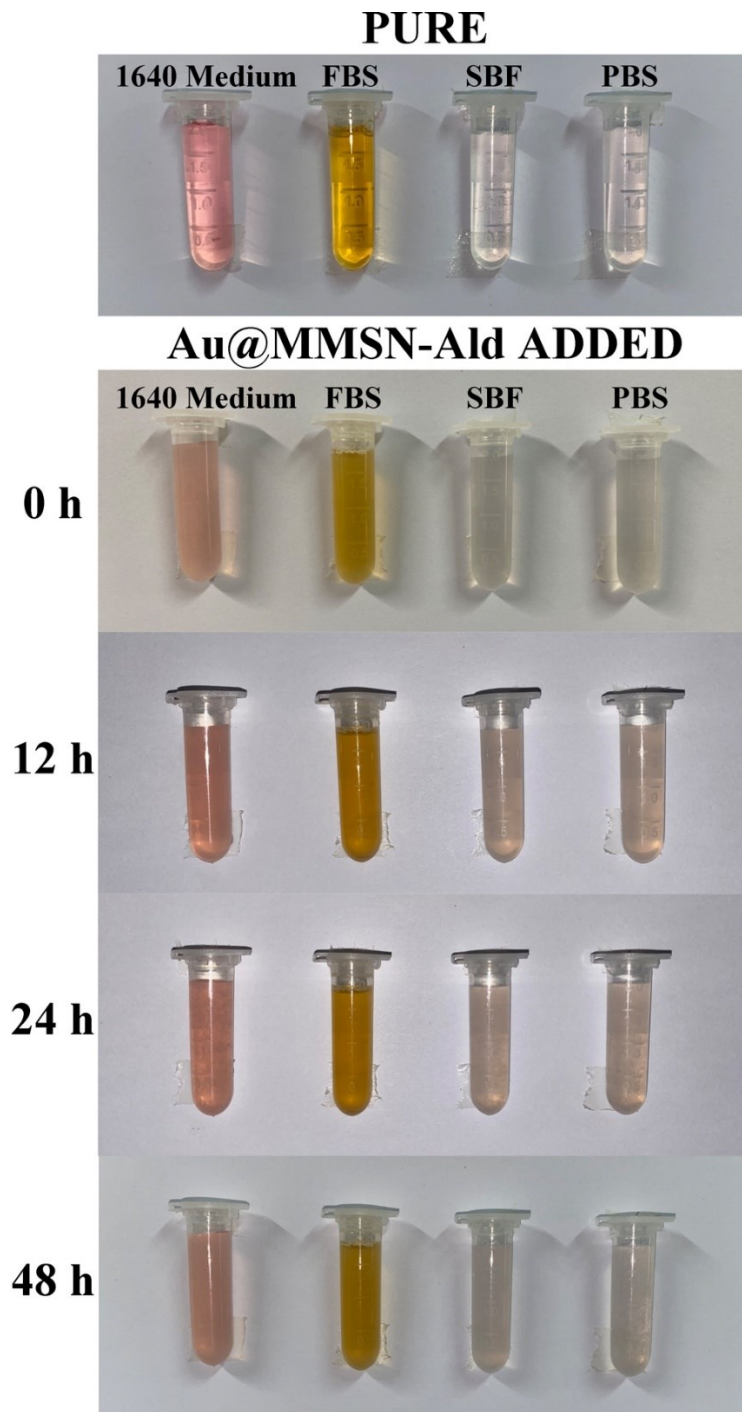


**Fig. S5** The stability of Au@MMSN-Ald in different solutions.

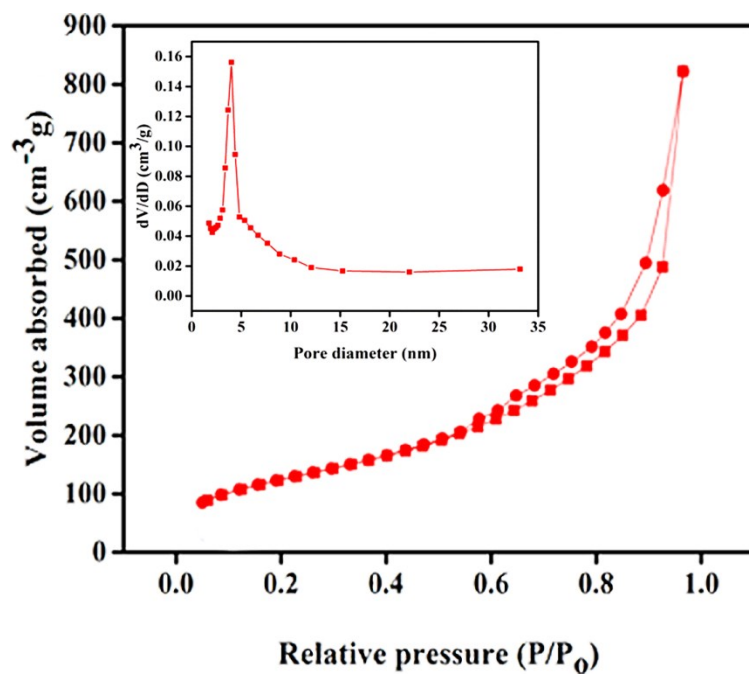


**Fig. S6** The N<sub>2</sub> absorption–desorption isotherm of Au@MMSN (inset: pore size distribution).

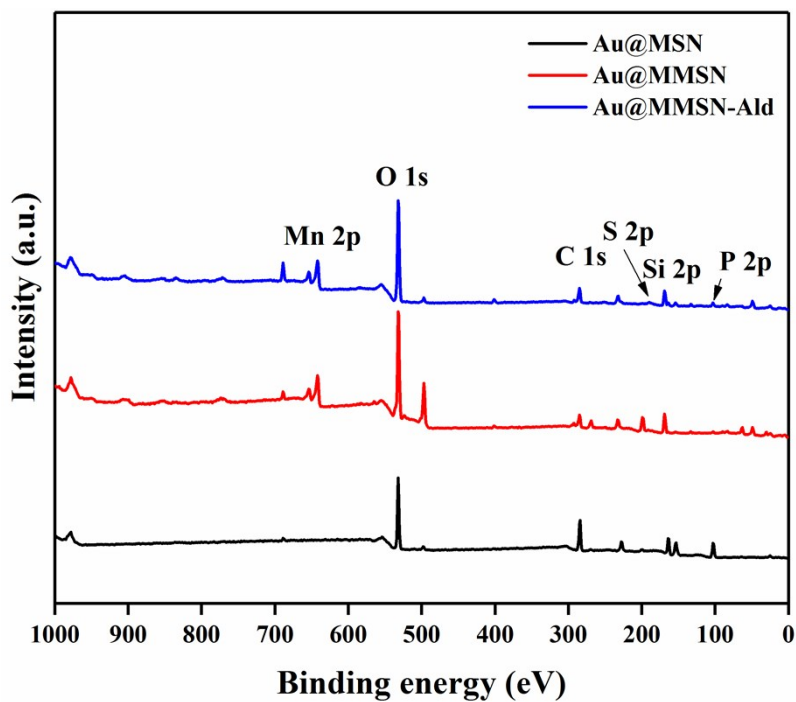


**Fig. S7** XPS spectra of Au@MSN, Au@MMSN and Au@MMSN-Ald.

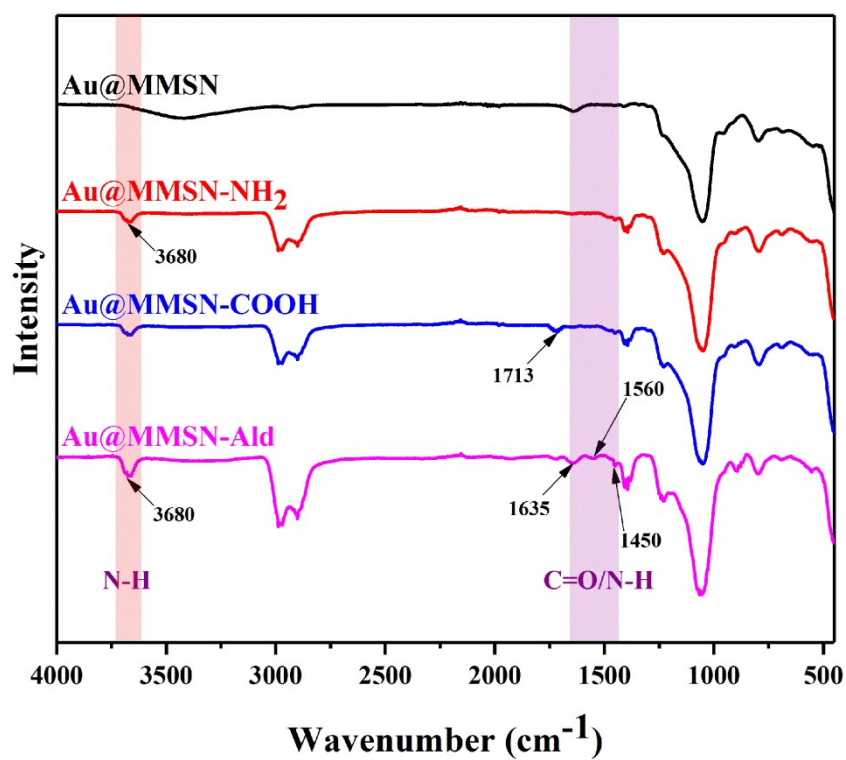


**Fig. S8** The FTIR spectra of Au@MMSN, Au@MMSN-NH<sub>2</sub>, Au@MMSN-COOH and Au@MMSN-Ald.

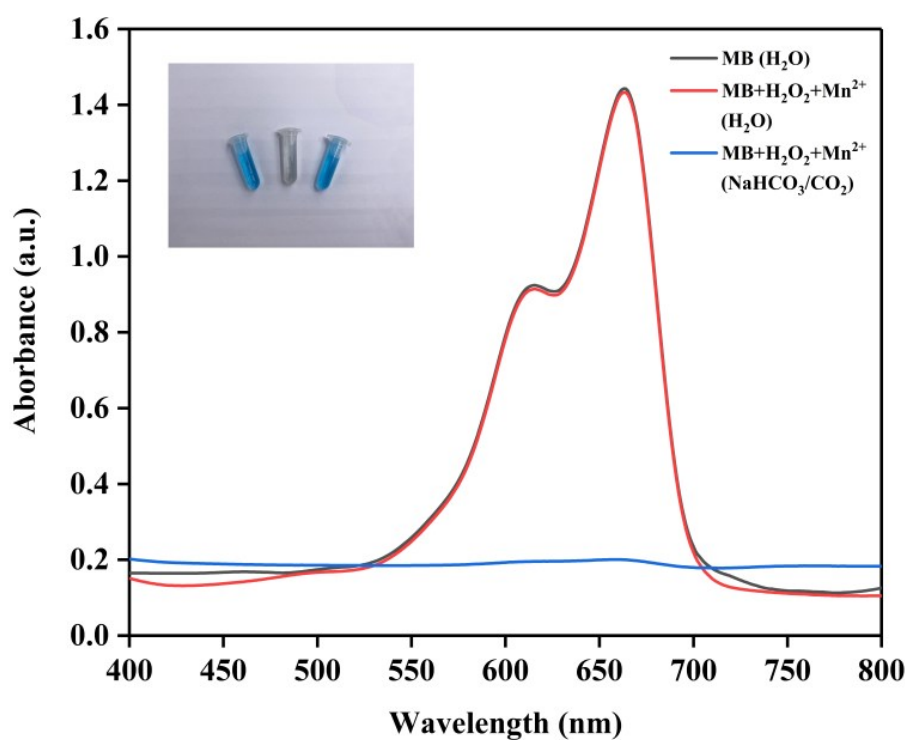


**Fig. S9** UV-Vis absorption spectra and photo (inset) of MB after degradation by the Mn<sup>2+</sup>-mediated Fenton-like reaction in different solutions.

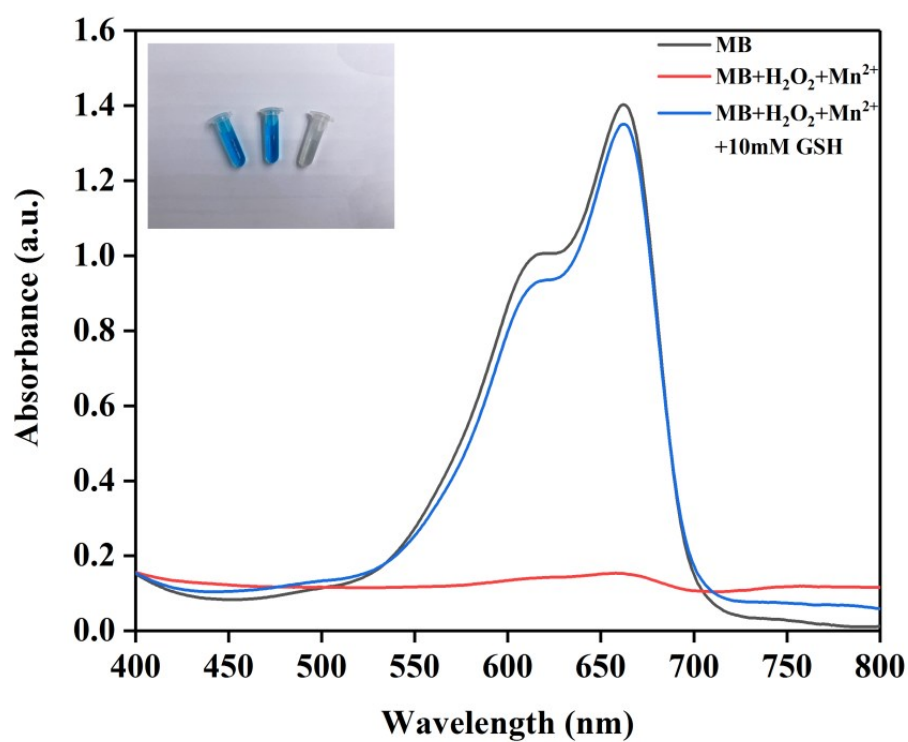


**Fig. S10** MB degradation by  $\text{Mn}^{2+}$ -mediated Fenton-like reaction in the presence or absence of GSH.

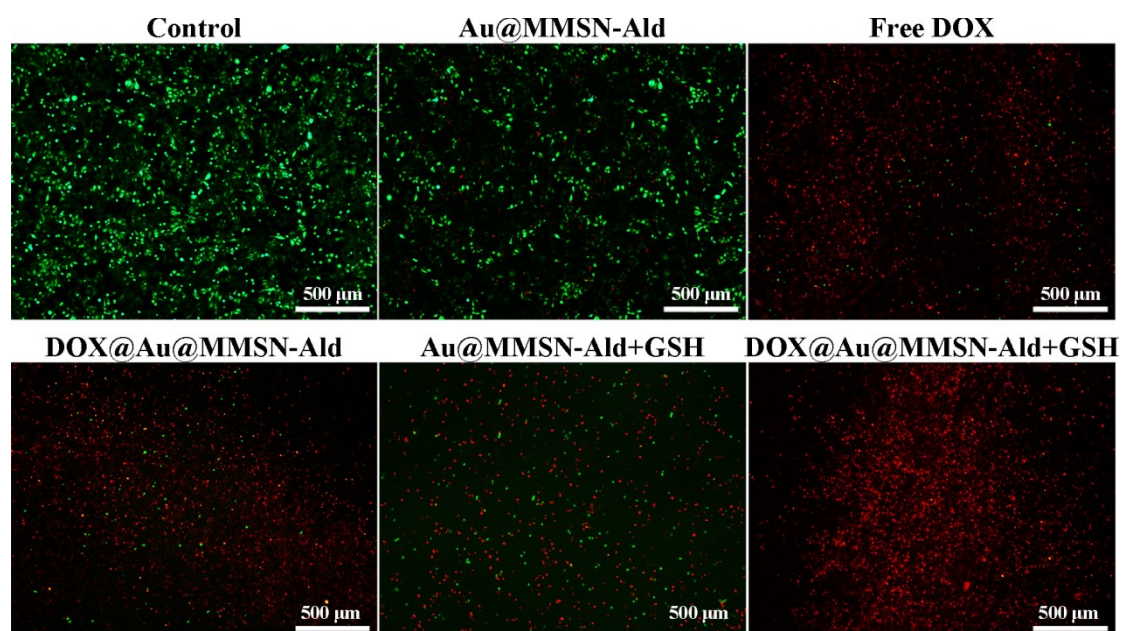


**Fig. S11** Fluorescence images of 143B cells stained with calcein-AM (green, live cells) and PI (red, dead cells) after different treatments.



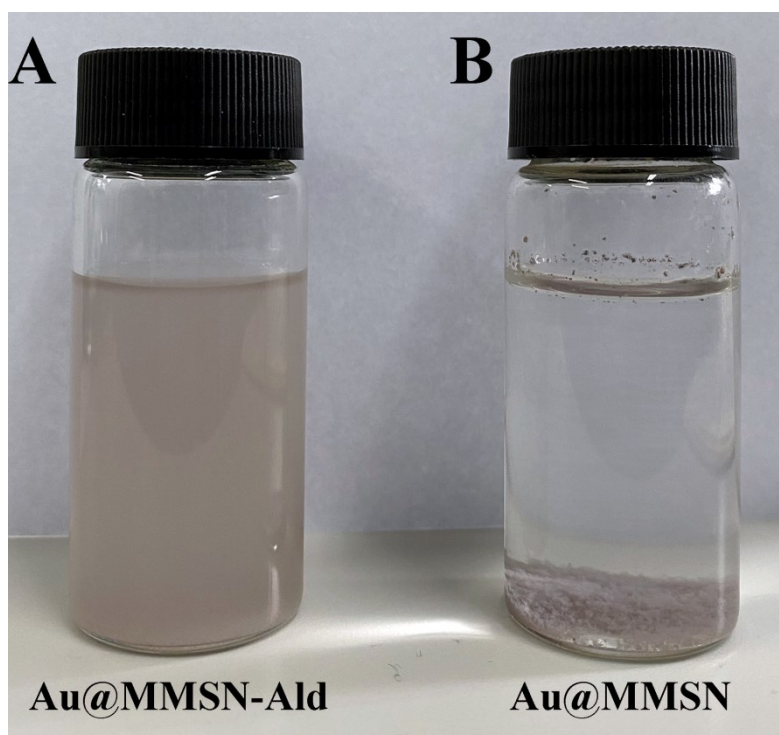


**Fig. S12** (A) Au@MMSN-Ald and (B) Au@MMSN dispersed in PBS for 1 h after ultrasonic treatment.

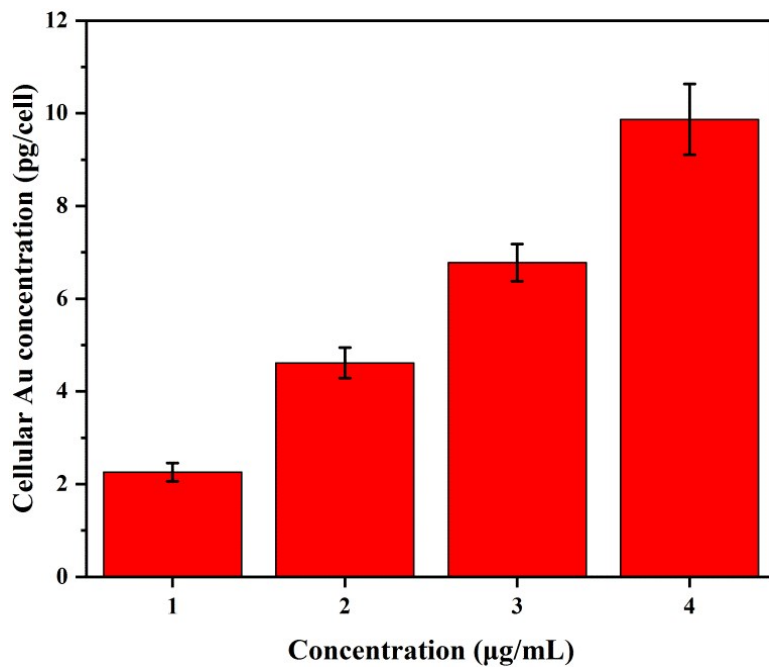


**Fig. S13** Cellular Au concentration in 143B cells after treated with different concentrations of Au@MMSN-Ald for 6 h.

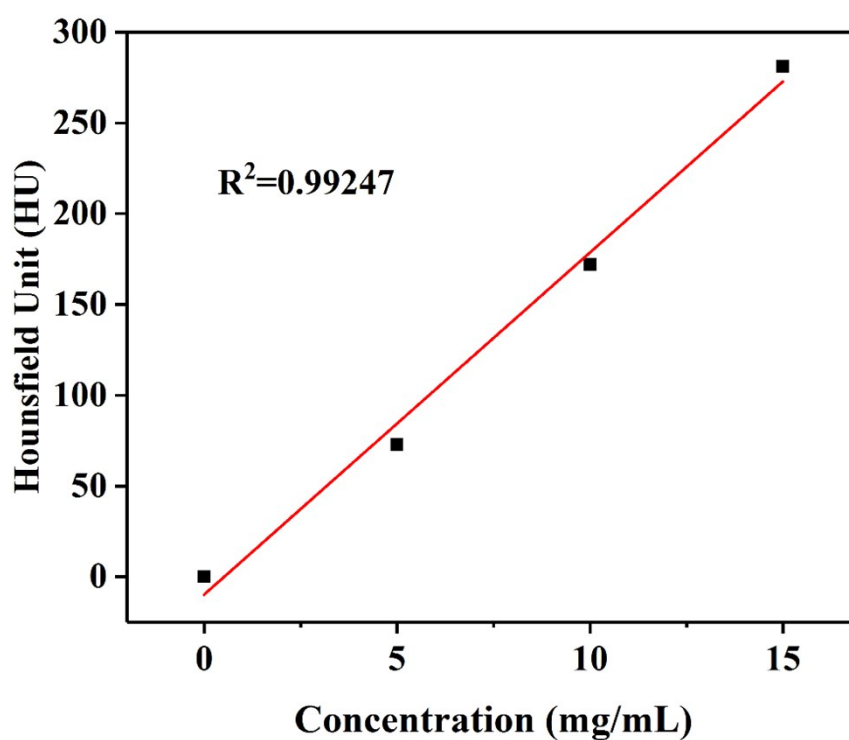


Fig. S14 X-ray attenuation intensity of the Au@MMSN-Ald at different concentrations.

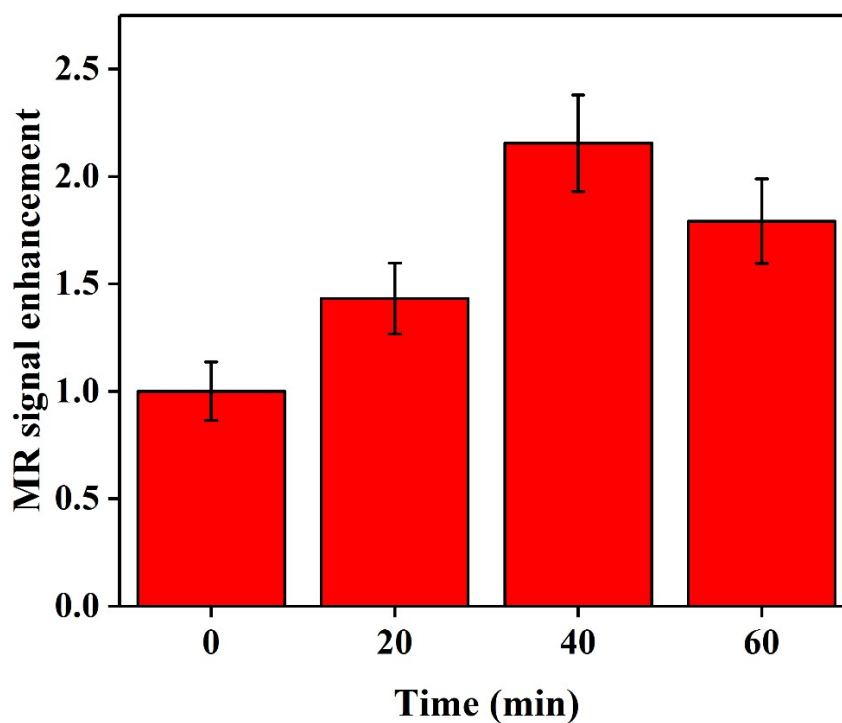


Fig. S15 The corresponding signal intensity enhancement of tumor region in MR imaging.

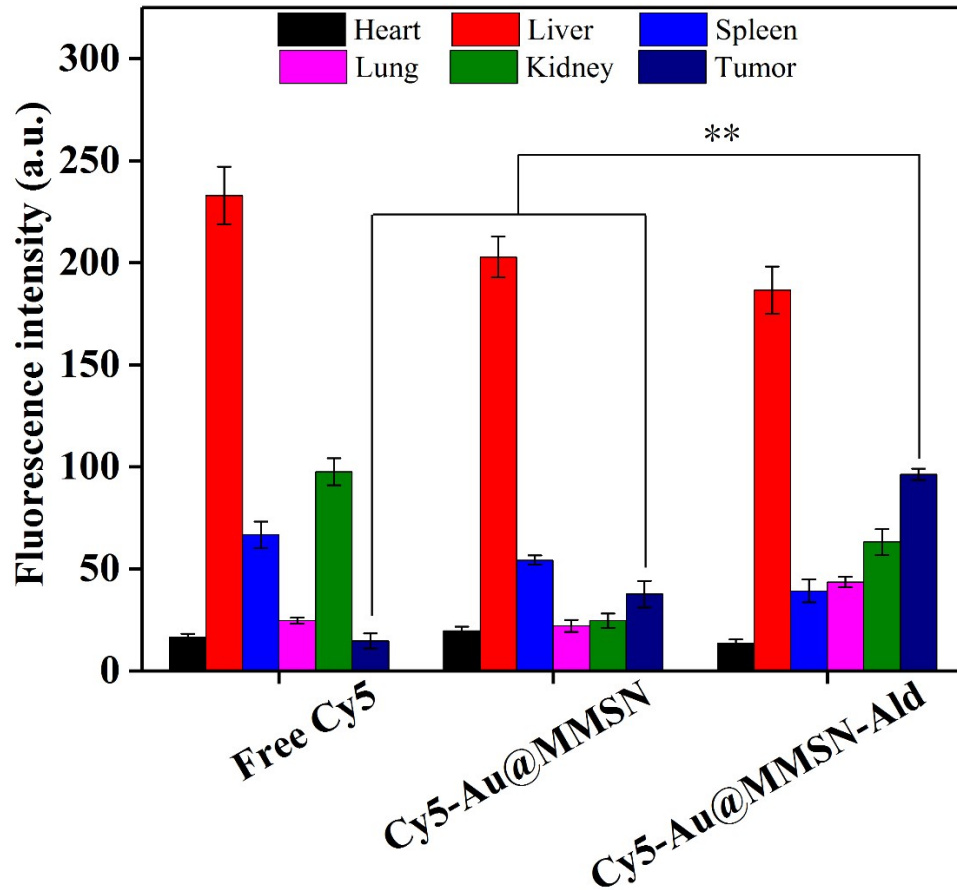


Fig. S16 The fluorescence intensity of organs to show the different nanoparticles retention at 6 h after intravenous injection.

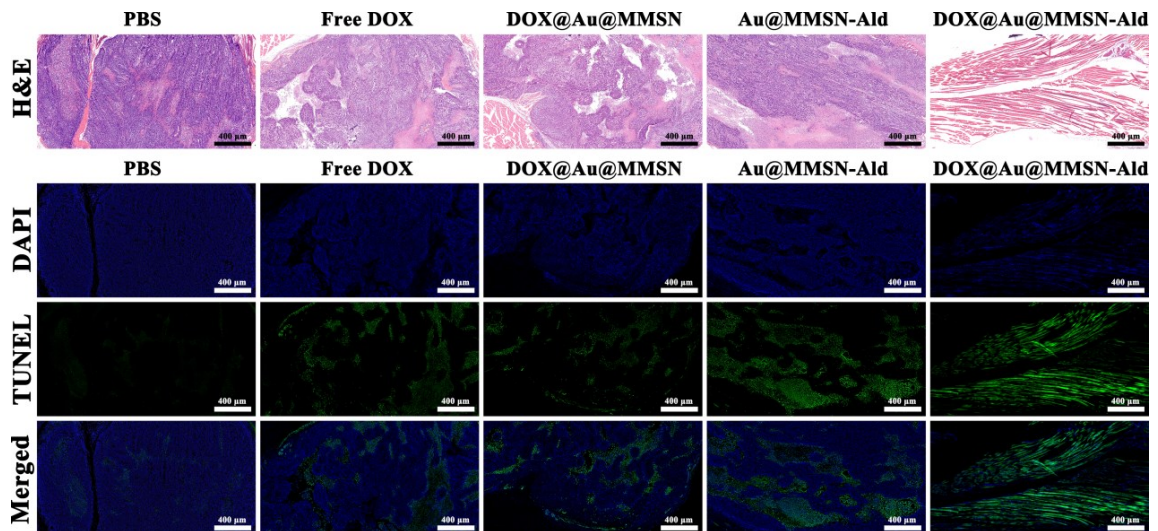


Fig. S17 H&E and TUNEL staining of tumor tissue after treatment with different groups.